Formation of thermal flow fields and chemical transport in air and water by atmospheric plasma

Formation of thermal flow fields and chemical transport in air and water by atmospheric plasma

Tetsuji Shimizu[1]**, Yutaka Iwafuchi**[2]**, Gregor E Morfill**[1]
and Takehiko Sato[3,4]

[1] Max-Planck Institute for Extraterrestrial Physics, 85748 Garching, Germany
[2] Graduate School of Engineering, Tohoku University, 2-1-1 Katahira, Aoba-ku, Sendai 9808577, Japan
[3] Institute of Fluid Science, Tohoku University, 2-1-1 Katahira, Aoba-ku, Sendai 9808577, Japan
E-mail: sato@ifs.tohoku.ac.jp

Abstract. Cold atmospheric plasma is a potential tool for medical purposes, e.g. disinfection/sterilization. In order for it to be effective and functional, it is crucial to understand the transport mechanism of chemically reactive species in air as well as in liquid. An atmospheric plasma discharge was produced between a platinum pin electrode and the surface of water. The thermal flow field of a cold atmospheric plasma as well as its chemical components was measured. A gas flow with a velocity of around $15\,\mathrm{m\,s^{-1}}$ to the water's surface was shown to be induced by the discharge. This air flow induced a circulating flow in the water from the discharge point at the water's surface because of friction. It was also demonstrated that the chemical components generated in air dissolved in water and the properties of the water changed. The reactive species were believed to be distributed mainly by convective transport in water, because the variation in the pH profile indicated by a methyl red solution resembled the induced flow pattern.

S Online supplementary data available from stacks.iop.org/NJP/13/053025/mmedia

[4] Author to whom any correspondence should be addressed.

IOP Institute of Physics ⬧ DEUTSCHE PHYSIKALISCHE GESELLSCHAFT

Contents

1. Introduction

Research on atmospheric plasma has led to the development of many applications, such as gas/water purification, coating and medicine [1, 2], because the atmospheric plasma system has many advantageous characteristics; for example, simple design, low cost and ease of handling [3]. Even in room-temperature plasma, many chemical reactions take place because the electron temperature is still high.

Recently, the field of 'plasma medicine' has attracted much interest because atmospheric plasma has been determined to have bactericidal and fungicidal properties [4]–[8]. Plasma has many advantages in that it enables contact-free, waste-free and local treatment, etc, and a wide range of plasma devices have been proposed and tested; for example, dielectric barrier discharge [9]–[11], surface micro-discharge [12], plasma jet [13]–[15] and plasma torch [16]–[19]. Reactive oxygen and nitrogen species are thought to mainly contribute to this biocidal property. Between the plasma and living tissues, in many cases there are ambient air and liquid. For instance, when chronic wounds are treated with cold atmospheric plasma [20, 21], these wounds are often covered by a body liquid, e.g. blood. Thus, it is important to understand the production and transport of reactive species generated by atmospheric plasma to the cells through air and liquid.

Atmospheric plasma is known to produce a gas flow [22, 23]. The ions in an electric field are accelerated and, through collisions, the momentum of ions is transferred to neutrals, resulting in a gas flow. Such a gas flow can enhance the mixing of reactive gases in liquid. Moreover, it can produce a flow in the liquid.

The aim of this study was to elucidate the production and transport of reactive species. Atmospheric plasma was produced between an electrode and the water's surface. Reactive species were produced in air and at the surface of water. Those species were dissolved in water. Flows as well as chemical components in air and water were examined.

2. Experimental setup

In principle, atmospheric plasma is produced by a streamer discharge, as shown in figure 1. The electrode system consists of a platinum rod of 0.3 mm diameter with a rounded edge and water in a glass cell with dimensions 20 mm × 10 mm × 8 mm. The 20 mm × 8 mm plane was mainly used in the following observations. Water (1.6 ml) was poured into the glass cell until the level
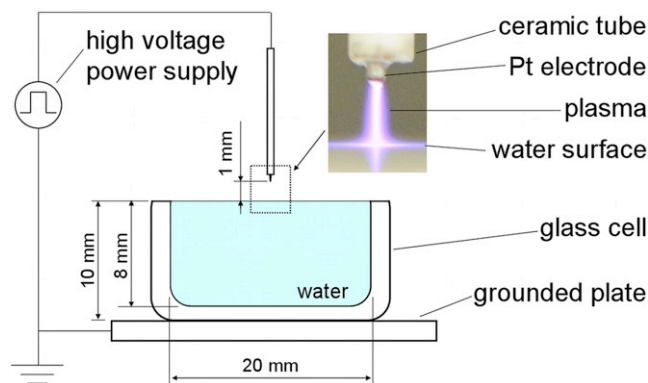
Figure 1. Electrode configuration. A discharge was produced between the tip of the Pt electrode and the water surface, as shown in the inset.

of the water's surface was as high as the glass cell. During our experiment, the evaporation of water was negligible. For example, after 5 min of operation, less than $10\,\mu$l of evaporation was observed. The tip of the platinum electrode was placed 1 mm above the water's surface vertically and covered by a ceramic tube except for the 0.5 mm discharge edge. The electrode and the glass cell were set in still atmospheric air and there was no injected gas flow. A metal plate was placed below the glass cell and electrically grounded. This circuit was capacitive and the capacitance was 0.8 pF measured by an LCR meter (Hioki, LCR HiTESTER 3535). By applying a high voltage of 7.5 kV_{0p} with a square wave (duty ratio 50%) at 5 kHz with respect to the ground (using a high-voltage amplifier; TREC, model PD05034), a plasma discharge was produced between the tip of the platinum electrode and the water's surface (see the inset of figure 1). The total power consumption was around 12 W (by the Lissajous technique with 1 μF capacitance).

The applied voltage was measured by a voltage monitor in the amplifier, while the electrical current was monitored by a current transformer (Pearson, model 6585). Both waveforms were recorded using an oscilloscope (LeCroy WaveSurfer 62Xi).

Video images of the density gradient in gas as well as in water were recorded using the Schlieren flow visualization technique, employing a high-speed camera, collimators, a knife-edge and a light source (online supplementary data available from stacks.iop.org/NJP/13/053025/mmedia). This method can be used to visualize a density variation in the flow of the fluid.

Microparticles of polymethylmethacrylate, 5 μm in diameter, were used for particle image velocimetry (PIV) for observing the flow pattern in water. The specific gravity of these particles was 1.2. The microparticles were distributed in water and their motion was visualized through the scattered light from a narrow laser sheet (532 nm wavelength), which illuminated a vertical plane of around 2 mm thickness passing through the cell.

In order to identify reactive species generated in the plasma gas, optical spectra measurement was carried out using an optical spectrometer (Hamamatsu PMA-12). Reactive species in the gas were observed using a gas detector (Dräger Multiwarn). A suction tube attached to the detector was placed in the vicinity of the plasma discharge and the concentrations of NO, NO_2 and CO were measured. For O_3 concentration, an ozone meter (SEKI Electronics, SOZ-3504) was used.
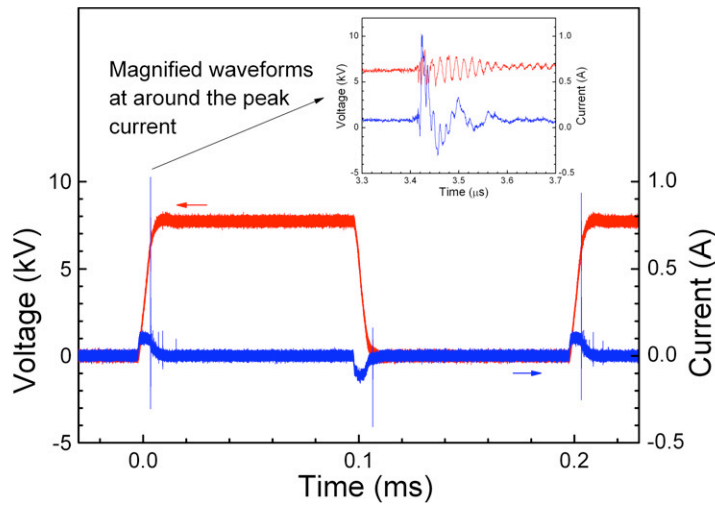
Figure 2. Waveforms of the applied voltage and current and magnifications of the waveforms at the peak current.

pH measurement was carried out using methyl red solution (Wako Pure Chemical Industries, reagent number 134-14121). The solution was dissolved in the water in the cell at a concentration of $2\,mg\,l^{-1}$. A change in color was observed by video camera. A change in color from yellow to red indicates a change in pH from 6.2 to 4.2. The pH of the water was measured by a pH meter (Eutech Instruments, PC6500). In addition, the concentrations of OH, O_3 and HNO_2 in water were estimated by using a water quality meter (Kyoritsu Chemical-Check Laboratories, DPM-MT). Here, the pH value (conductivity) of the pure water and the solution before plasma treatment were 6.7 ($1.3\,\mu S\,cm^{-1}$) and 6.8 ($23.5\,\mu S\,cm^{-1}$), respectively.

Water temperature was measured by a 0.08 mm E-type thermocouple. At positions 1 mm from the surface and at positions 1 mm from the bottom of the water, the temperatures were measured following certain discharge times. For each measurement, the water was changed during these temperature measurement experiments.

3. Experimental results and discussion

3.1. Plasma characteristics and thermal flow field in air

Figure 2 shows the typical waveforms of the applied voltage and current. Magnifications of the waveforms at around the peak current are shown in the inset of figure 2. When the applied voltage reaches the breakdown voltage, the current grows rapidly and a plasma discharge is produced between the electrode and the water's surface. A displacement current of approximately 0.2 A due to the capacitance of the system and a peak current of approximately 1 A are responsible for the discharge. During the discharge, charge is accumulated in the water, terminating the discharge. The full-width at half-maximum of the current in our particular experiment was around 20 ns. About $10\,\mu s$ after this increase in current, small peaks were observed. These peaks correspond to several discharges between the lower part of the cell and the ground plate. When the applied voltage dropped to 0 V, a sharp peak in the current waveform was again observed.
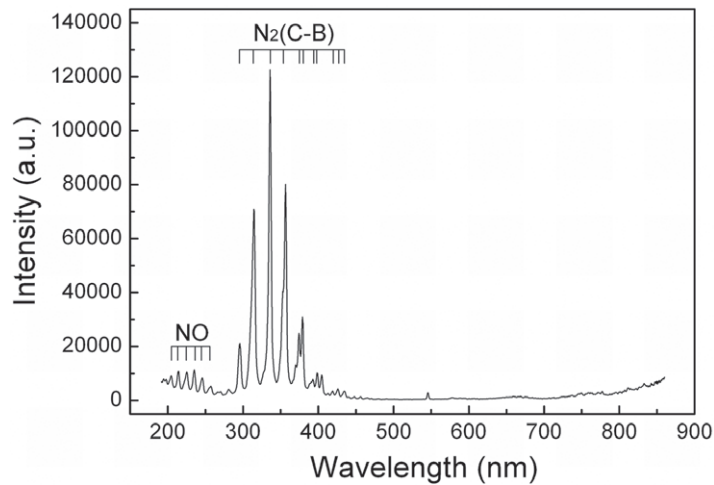
Figure 3. Optical spectrum from the plasma discharge. In UV, one can observe peaks from N_2 and NO.

Figure 3 shows the optical spectrum of the plasma discharge. In UVA and UVB, there are several peaks corresponding to the N_2 second positive system. In UVC, several peaks could be observed corresponding to the NO γ system [24]. From the peaks of the N_2 second positive system, the rotational temperature in the plasma discharge was estimated to be around 2000 K [25]–[28]. The rotational temperature shows the same temperature range (1600–3500 K) as that reported in previous studies [29]–[32]. The measurements by the gas detector were ~ 10 ppm of NO_2, ~ 1 ppm of NO, ~ 2 ppm of CO and ~ 16 ppm of ozone. Production of reactive species in the plasma gas was obvious.

Schlieren visualization revealed the density variation in the plasma flow, as shown in figure 4. Images were recorded every $16 \, \mu$s. Because the signal in the images was very faint, the difference between each image and the same image before the start of plasma discharge was calculated for all of the frames in the movie file in order to make the signal clear to see. At $t = 0$ s, the plasma discharge was initiated and then the images were shown every $16 \, \mu$s. These images were thought to be recorded when the voltage dropped from 7.5 kV to 0 V. We have already confirmed that the images of a discharge with a voltage rise were very similar to those with a voltage drop. In this case, the temperature field is given on the images since pressure is constant in this experiment. Note that this plasma was produced in open air. Immediately after the start of discharge, a hot spot was created in the vicinity of the electrode tip. Afterwards, the hot region extended to the water's surface at $t = 16 \, \mu$s, presumably because the neutral gas in the plasma discharge was heated by ions that were locally distributed. Almost simultaneously, a crescent-shaped hot region was produced and this region was transported to the water's surface at a velocity of around 15 m s^{-1}. This transport was apparently driven by accelerated ions in the electric field [23]. Around the platinum electrode, the electric field was stronger owing to the shape.

3.2. Thermal flow field and chemical transport in water

First, the flow pattern was measured by means of the PIV method, as shown in figure 5. The flow pattern appears to be a circulating flow. The initial flow was induced at the discharge point at the
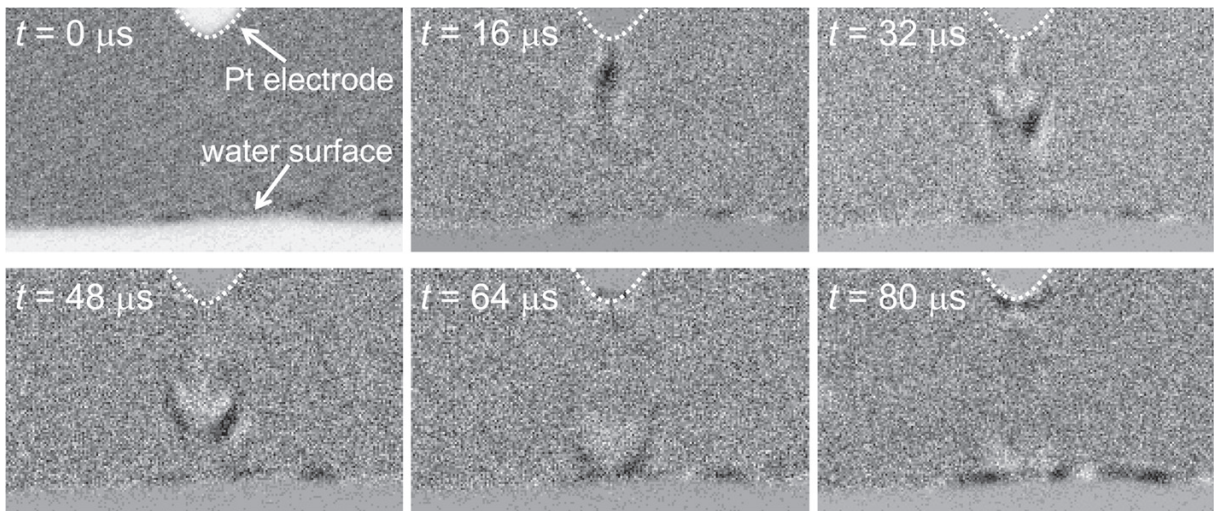
Figure 4. Density variation in the air between the electrode and the water's surface. A white dashed line shows the edge of the Pt electrode. At $t = 0$ s, plasma discharge was initiated.
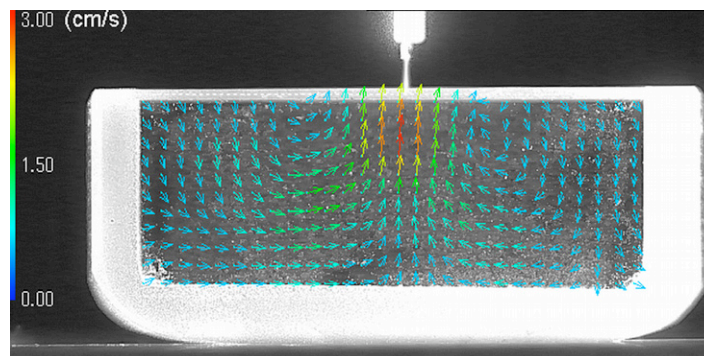

Figure 5. Typical velocity vector field in water measured by the PIV method. Particles of polymethylmethacrylate, 5 μm in diameter, were used.

surface of the water and this variation spread throughout the water. At the surface of the water, analysis was not possible because of light reflection from the edge of the cell. From the velocity vector field around the ends of the cell, it was believed that there is a horizontal fast flow on the surface. Therefore, the flow speed in the vicinity of the surface was faster than that at the bottom. The maximum velocity of 2.5–3 cm s^{-1} was found at the center with upward direction in this analysis.

Next, the Schlieren visualization technique was applied to the analysis of the thermal field in water. Figure 6 shows a time series of images in the water. As mentioned before, a gas flow to the water's surface at the discharge point was induced. This is thought to drive the flow along the water's surface. Due to friction, the water was driven to follow the gas flow above the surface. As shown in figure 5, a thermal field started to build up along the water's surface. Afterwards, the thermal field developed a temperature difference with downward direction when this thermal field reached the wall of the cell ($t = 0.3$ s). At $t = 0.7$ s, the direction of the thermal
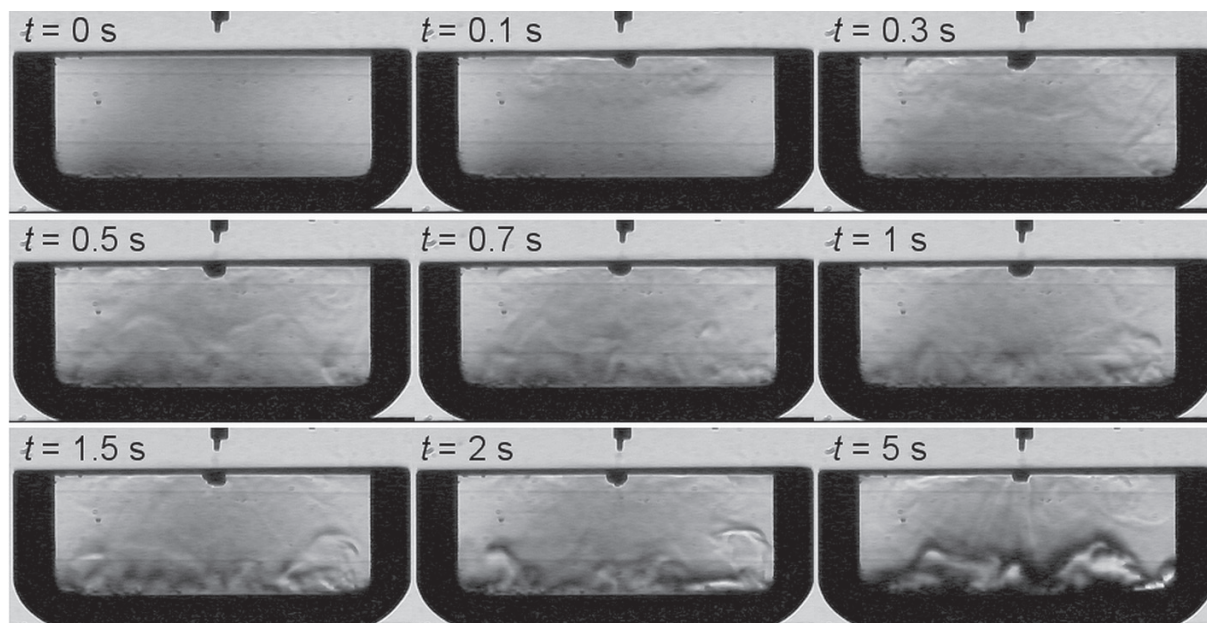
Figure 6. Thermal field in the water measured by the Schlieren method. At $t = 0$ s, plasma discharge was initiated.

field changed to the upward direction and a circulating flow was thought to be produced. Note that there are several sources capable of producing a thermal field from the bottom of the cell, especially at the lower corners of the cell. This is due to other discharges produced between the outside of the cell and the grounded plate. Measurements of the water temperature by the thermocouple showed that the average water temperature increased by about 10 K in 120 s, and at 120 s, the temperature at the top was 4 K higher than that at the bottom of the water. This indicates that natural convection was suppressed by the induced circulating flow and the thermal field pattern was mainly produced by the flow from the discharge. The shape of this result looks quite similar to that of the flow measured by the PIV method. From this measurement, we believe that the thermal field pattern also represents the flow.

In order to see a change in the water, a solution of methyl red was treated by plasma discharge. Figure 7 shows the temporal evolution of color change in the methyl red solution. At $t = 0$ s, production of the discharge began. At $t = 1$ s, around the plasma discharge point, the color had already begun to change from yellow to red, and as t increased, the red region expanded to the entire cell. At $t = 30$ s, the entire solution turned red. The color change was confirmed to be due to the change in pH of the water, and we believe that the denaturation of methyl red can be excluded through our series of tests. The discoloration looks similar to the flow pattern already discussed above. For instance, at $t = 5$ s, the yellow region has a conical shape and this shape is very similar to the flow pattern measured by the PIV method shown in figure 5. This suggests that some components that can change the pH were transported in the water, followed by the flow induced by the plasma discharge [33]–[35].

The discoloration, in other words the decrease in pH, is thought to be caused by dissolution of chemical components produced by the plasma discharge. As mentioned before, reactive species are produced in the gas and these species can dissolve in water. Figure 8 shows the concentrations of H_2O_2, O_3 and HNO_2 in the treated water as a function of the discharge time t.
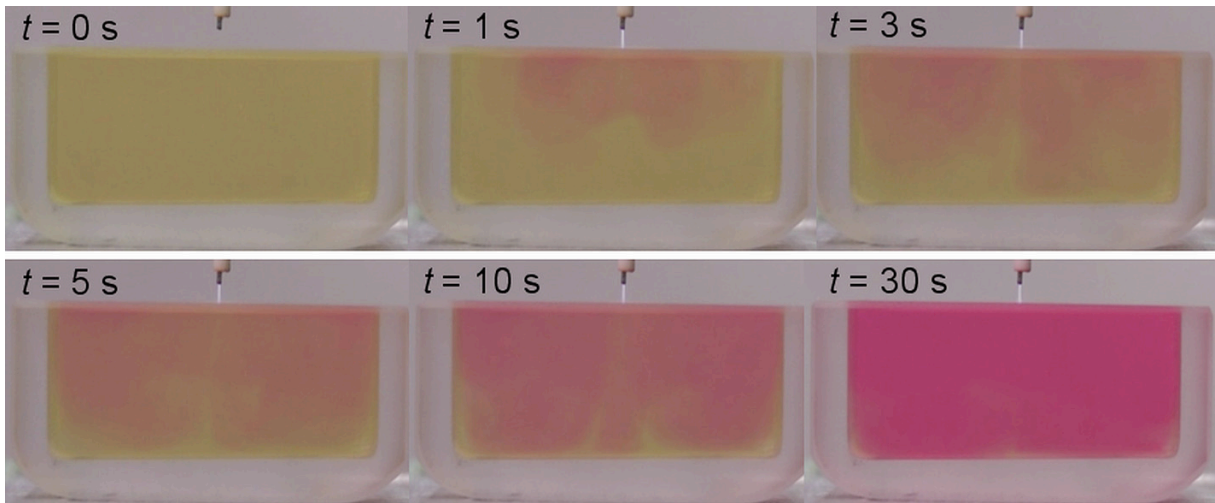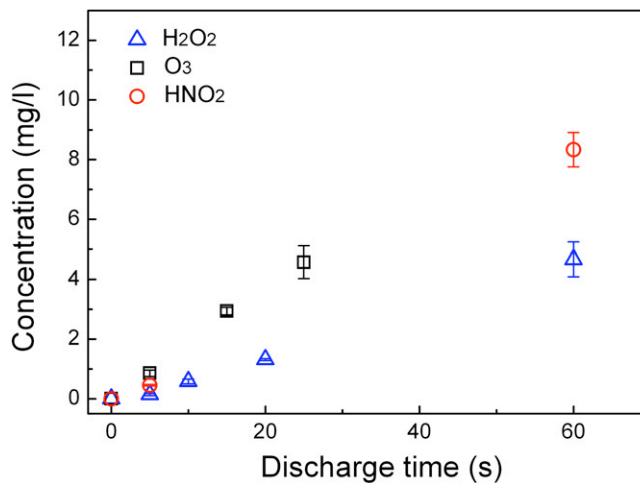
Figure 7. Temporal change in water with methyl red.

Figure 8. Concentrations of H_2O_2, O_3 and HNO_2 in water as a function of discharge time t.

As the discharge time increases, the concentration of all of the species increases. The decrease in pH is thought to be caused by the dissolution of NO_x. If NO_x is dissolved in water, nitric acid can be produced, resulting in a drop in pH.

Let us demonstrate the flow in the air and water to facilitate an understanding of the chemical transport. In the field of plasma medicine, reactive oxygen and nitrogen species are very important with regard to bactericidal processes [6]. This bactericidal property is thought to depend on multiple processes, i.e. cell permiabilization [36, 37], penetration of reactive species into the cell, reaction with the cytoplasm, etc. Therefore, it is crucial to tune the chemical components from the plasma discharge to the cells. For instance, plasma-treated liquid can be toxic to bacteria but it has no adverse effect on human skin fibroblast viability and migrations by tuning the chemical components [38]. The authors have previously proposed that this effect can be attributed to the synergy of plasma-generated nitric oxide and hydrogen peroxide [38].

IOP Institute of Physics ⊕ DEUTSCHE PHYSIKALISCHE GESELLSCHAFT

Moreover, Ikawa *et al* [39] have reported that the pH of a liquid treated by plasma discharge is a very important parameter for the bactericidal property. The present authors have previously reported that there was a threshold of pH for the bactericidal effect due to the equilibrium between superoxide anion radicals and hydroperoxy radicals [39]. For the optimization of the plasma discharge depending on requirements, it is important to tune both the produced chemically reactive species and the pH of the liquid. Since plasma treatment results in a change in the pH of a liquid and this change starts to propagate in the liquid from the point of contact with the discharge, it is important to design the shape of the discharge above the liquid. In the case of a smaller depth of water, the effect of gas flow might be less and the induced velocity is reduced by the viscosity. However, it is considered that a circular flow could still be induced in water.

4. Summary

In order to understand the transport mechanism of reactive species in air as well as in water, the thermal flow field and transport of chemical components were measured with a Pt electrode–water surface dielectric barrier discharge system. An air flow of $15\,\mathrm{m\,s^{-1}}$ was found to be driven by the discharge towards the water's surface and this flow induced a flow of $3\,\mathrm{cm\,s^{-1}}$ at the center with upward direction in the water. The flow in the water has a circulating pattern and the change in pH is followed by induced flow in the water. With this change, the dissolution of chemically reactive species, such as HNO_2, was also observed, resulting in a decrease in pH in the water. The discoloration of the methyl red solution progressed along with the flow pattern; thus it is suggested that chemical components are transported by convection, which is induced by the discharge. These phenomena are considered to be important to understand the processes in a liquid, e.g. the mechanism of the inactivation of bacteria in a liquid.

Acknowledgments

References

[1] Bruggeman P and Leys C 2009 *J. Phys. D: Appl. Phys.* **42** 053001
[2] Locke B R, Sato M, Sunka P, Hoffmann M R and Chang J-S 2006 *Ind. Eng. Chem. Res.* **45** 882
[3] Park J, Henins I, Hermann H W, Selwyn G S and Hicks R F 2001 *J. Appl. Phys.* **89** 20
[4] Stoffels E 2007 *Contrib. Plasma Phys.* **47** 40
[5] Fridman G, Shekhter A B, Vasilets V N, Friedman G, Gutsol A and Fridman A 2008 *Plasma Process. Polym.* **5** 503
[6] Laroussi M 2002 *IEEE Trans. Plasma Sci.* **30** 1409
[7] Kong M G, Kroesen G, Morfill G E, Nosenko T, Shimizu T, Dijk van J and Zimmermann J L 2009 *New J. Phys.* **11** 115012
[8] Weltmann K D, Kindel E, von Woedtke T, Haehnel M, Stieber M and Brandenburg R 2010 *Pure Appl. Chem.* **82** 1223

[9]   Sato T, Furuya O, Ikeda K and Nakatani T 2008 *Plasma Process. Polym.* **5** 606
[10] Fridman G, Peddinghaus M, Ayan H, Fridman A, Balasubramanian M, Gutsol A, Brooks A and Friedman G 2006 *Plasma Chem. Plasma Process.* **26** 425
[11] Boudam M K, Moisan M, Saoudi B, Popovici C, Gherardi N and Massines F 2006 *J. Phys. D: Appl. Phys.* **39** 3494
[12] Morfill G, Shimizu T, Steffes B and Schmidt H-U 2009 *New J. Phys.* **11** 115019
[13] Walsh J L, Shi J J and Kong M G 2006 *Appl. Phys. Lett.* **88** 171501
[14] Laroussi M, Tendero C, Lu X, Alla S and Hynes W L 2006 *Plasma Process. Polym.* **3** 470
[15] Weltmann K D, Brandenburg R, von Woedke T, Ehlbeck J, Forest R, Stieber M and Kindel E 2008 *J. Phys. D: Appl. Phys.* **41** 194008
[16] Sato T, Miyahara T, Doi A, Ochiai S, Urayama T and Nakatani T 2006 *Appl. Phys. Lett.* **89** 073902
[17] Miyahara T, Ochiai S and Sato T 2009 *Euro. Phys. Lett.* **86** 45001
[18] Sato T, Ochiai S and Urayama T 2009 *New J. Phys.* **11** 115018
[19] Shimizu T *et al* 2008 *Plasma Process. Polym.* **5** 577
[20] Isbary G *et al* 2010 *Br. J. Dermatol.* **163** 78
[21] Heinlin J, Morfill G, Landthaler M, Stolz W, Isbary G, Zimmermann J, Shimizu T and Karrer S 2010 *J. Deutschen Dermatol. Gesellschaft* **12** 968
[22] Loeb L 1965 *Electrical Corona* (Berkeley: CA: University of California Press)
[23] Boeuf J P, Lagmich Y, Callegari Th and Pitchford L C 2007 *J. Phys. D: Appl. Phys.* **40** 652
[24] Pearse R W B and Gaydon A G 1950 *The Identification of Molecular Spectra* (New York: Wiley)
[25] Yuji T, Suzaki Y, Yamawaki T, Sakaue H and Akatsuka H 2007 *Japan. J. Appl. Phys.* **46** 795
[26] Sakamoto T, Matsuura H and Akatsuka H 2007 *J. Appl. Phys.* **101** 023307
[27] Sakamoto T, Matsuura H and Akatsuka H 2006 *Japan. J. Appl. Phys.* **45** 7905
[28] Koike S, Sakamoto T, Kobori H, Matsuura H and Akatsuka H 2004 *Japan. J. Appl. Phys.* **43** 5550
[29] Bruggeman P, Ribězl E, Maslani A, Degroote J, Malesevic A, Rego R, Vierendeels J and Leys C 2008 *Plasma Sources Sci. Technol.* **17** 025012
[30] Lu X-P and Laroussi M 2005 *IEEE Trans. Plasma Sci.* **33** 272
[31] Titov V A, Rybkin V V, Smirnov S A, Kulentsan A L and Choi H-S 2006 *Plasma Chem. Plasma Process.* **26** 543
[32] Bruggeman P, Schram D C, Kong M G and Leys C 2009 *Plasma Process. Polym.* **6** 751
[33] Helmke A, Hoffmeister D, Mertens N, Emmert S, Schuette J and Vioel W 2009 *New J. Phys.* **11** 115025
[34] Oehmigen K, Haehnel M, Brandenburg R, Wilke Ch, Weltmann K-D and von Woedtke Th 2010 *Plasma Process. Polym.* **7** 250
[35] Liu F *et al* 2010 *Plasma Process. Polym.* **7** 231
[36] Leduc M, Guay D, Leask R L and Coulombe S 2009 *New J. Phys.* **11** 115021
[37] Yonson S, Coulombe S and Leask R L 2006 *J. Phys. D: Appl. Phys.* **39** 3508
[38] Nosenko T, Shimizu T and Morfill G 2009 *New J. Phys.* **11** 115013
[39] Ikawa S, Kitano K and Hamaguchi S 2010 *Plasma Process. Polym.* **7** 33